30 Mar 2001, 4:30 pm - 6:30 pm

Dynamics SSI Analyses Considering Anisotropy of the Foundation Gravelly Layer in Hualien, Taiwan

Yukihisa Tanaka

Central Research Institute of Electric Power Industry, Japan

DYNAMIC SSI ANALYSES CONSIDERING ANISOTROPY OF THE FOUNDATION GRAVELLY LAYER IN HUALIEN, TAIWAN

Yukihisa Tanaka
Central Research Institute of Electric Power Industry
Abiko City, Chiba Prefecture, Japan

ABSTRACT

The Hualien Large-Scale Seismic Test program is under way to investigate Soil-Structure Interaction during large earthquakes in the field of Hualien, a high seismic region in Taiwan. In this paper, the ground of the test site, which consists of a sand layer and a hard gravelly layer, was characterized and modeled for accurate dynamic simulation analysis. Especially, the anisotropic behavior of the gravelly layer is modeled and simulation analysis of the forced vibration test is conducted. Consequently, it was revealed that anisotropic behavior of the gravelly layer observed in earthquake observation and forced vibration tests could be expressed by the orthotropic elastic body model.

INTRODUCTION

An international joint program, the Hualien Large-Scale Seismic Test (called HLSST for short) program, is under way to investigate soil-structure interaction during large earthquakes in Hualien, a region in Taiwan of high seismicity.

A 1/4-scale model building was constructed on the gravelly soil layer in this site. Forced vibration tests (called FVT for short) of the model building before and after backfilling and earthquake observation of the soil-structure system were conducted. Extensive geotechnical investigation including velocity logging and sampling by the in-situ freezing technique was conducted for accurate evaluation of FVT and earthquake-induced response of the model building and surrounding ground. In this paper, anisotropic behavior of the gravelly soil layer observed in forced vibration test and in earthquake response is modeled by an orthotropic elastic body.

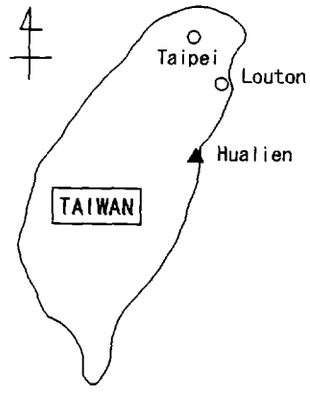

Fig.1 Location map of Hualien site

GEOTECHNICAL CHARACTERISTICS OF THE HUALIEN SITE

Outline of site investigation

Some results of the HLSST have already been reported (Morishita et al., 1993 ; Yamaya et al., 1995 ; Sugawara et al., 1997 ; Kokusho et al., 1997 ; Ueshima et al., 1996 ; Ueshima et al., 1997). Thus this paper focuses on the results of site investigation which are considered to be helpful to understand the peculiar characteristics of the gravelly layer described later.

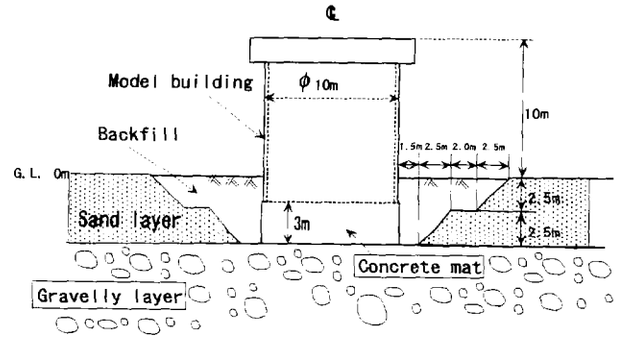

Fig.2 Outline of model building and surrounding ground (quoted from Kokusho et al. (1997) and modified)

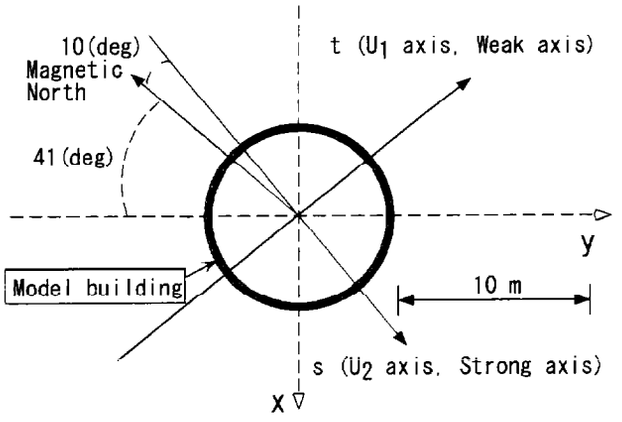

Fig.3 Direction of axes around the model building

Figure 1 shows the location of Hualien in Taiwan. Figure 2 is a rough cross section of the model building and its surrounding ground. The model building is cylindrical and a 1/4-scale model of the actual object. The model building is constructed on the surface of the gravelly layer, which is reportedly the Milun Formation of diluvial origin, at G.L.-5m after excavating the surface sand layer of diluvial origin. The model building is surrounded by compacted backfill of crushed stone.

Construction process of the model building is divided into the following four stages ;

Stage 1 : Before excavation
Stage 2 : After excavation and before constructing the model building
Stage 3 : After constructing the model building and before backfilling
Stage 4 : After backfilling

Velocity logging was conducted at each stage of construction mentioned above, while FVT of the model building was conducted at Stage 3(FVT1) and Stage 4(FVT2).

Figure 3 shows directions of the axes, which will be described in the later part of this paper, in a ground plan.

Velocity logging (Kokusho et al., 1997)

The velocity logging at Stage 1 was conducted by the down hole method and the cross hole method.

Figures 4(a) and 4(b) show the distribution of shear wave velocity by velocity logging conducted at Stage 1 together with the shear wave velocity evaluated by other methods. The shear wave velocity of the sandy layer from about G.L. -3 m to about G.L. -5 m is in the region of about 180 m/s ~ 220 m/s. The shear wave velocity of the gravelly layer of G.L. -5 m to -12 m by the down hole method as well as the cross hole method varies widely from about 300 m/s to about 400 m/s.

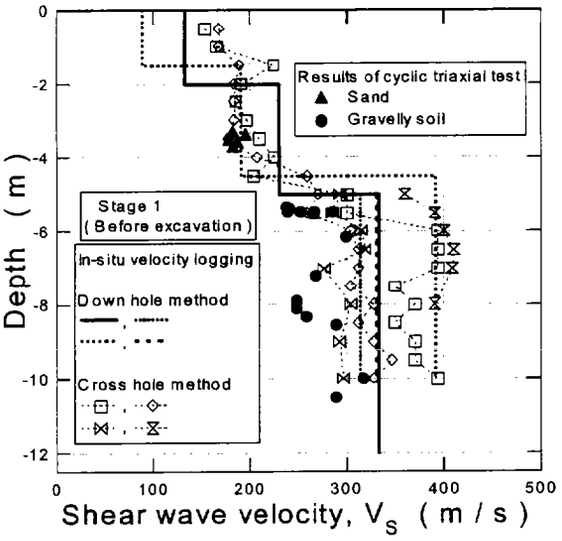

(a) Results of velocity logging and cyclic triaxial test

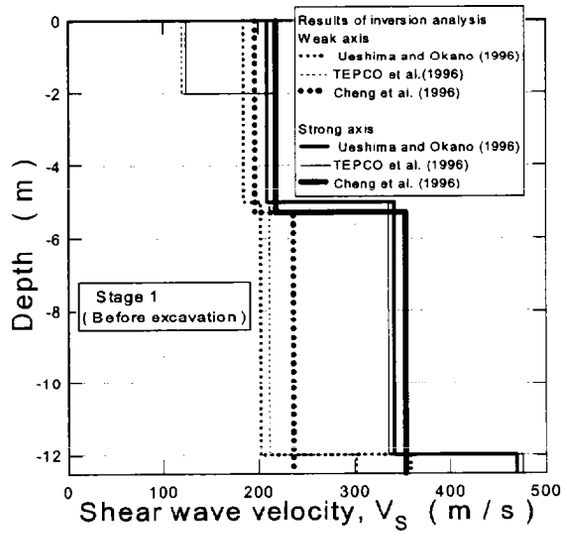

(b) Results of inversion analysis

Fig.4 Distribution of shear wave velocity at Stage 1 (Befo excavation)

Identification of shear wave velocity of soil by inversio analysis

In Fig.4(b), shear wave velocities identified b one-dimensional inversion analysis of observed earthquake a Stage 1 (Ueshima et al., 1996 ; Chen et al., 1996 ; TEPC group and Kajima research institute, 1996) are plotted. In tha case, all of the earthquakes used for the inversion analysis wer so small that nonlinearity of the ground could be ignorec Figure 4(b) indicates that the identified shear wave velocity c the sandy layer from G.L.-3 m to -5 m is almost independer of azimuth of the acceleration record coinciding with th

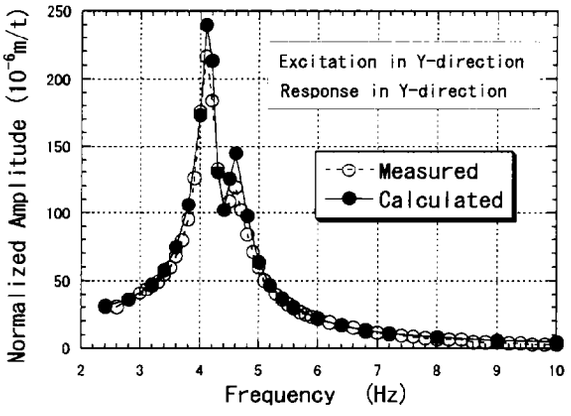

(a) Response in Y-direction

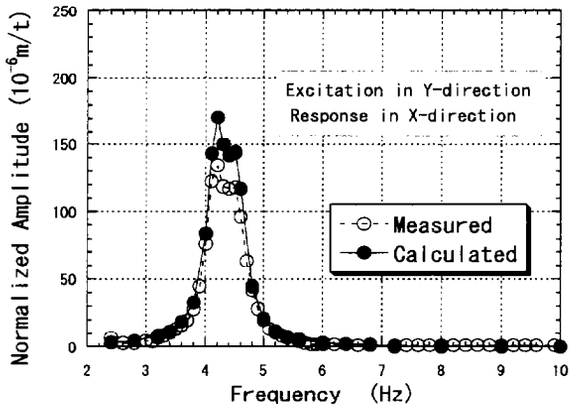

(b) Response in X-direction

Fig.5 Experimental Results of FVT1 and results of calculation (quoted from Yamaya et al. (1995) and modified)

results of velocity logging, whereas that of the gravelly layer below G.L. -5m shows obvious azimuth dependency.

Results of the FVT at Stages 3 and 4

At Stage 3 and Stage 4, FVT was conducted. The methodology of the FVT was described in literature (Morishita et al., 1993 ; Sugawara et al., 1997). Open circles in Figs. 5 and 6 denote the results of the FVT at Stages 3 and 4, respectively. In that case, a shaker was placed on the roof floor of the model building. The y-direction and x-direction are illustrated in Fig.3.

Each experimental resonance curve in Figs.5(a) and 5(b) has double peaks, whereas each experimental curve in Figs.6(a) and 6(b) has a single peak. Considering that the model building was without backfill at Stage 3 and that the model building is almost axisymmetric, the double peaks in Figs.5(a) and 5(b) are mainly attributable to the characteristics of the gravelly layer just beneath the model building.

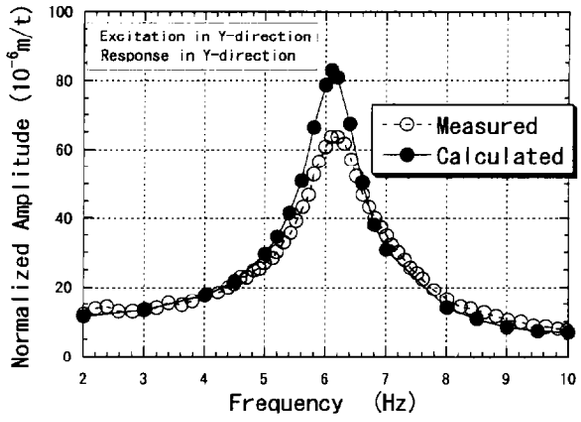

(a) Response in Y-direction

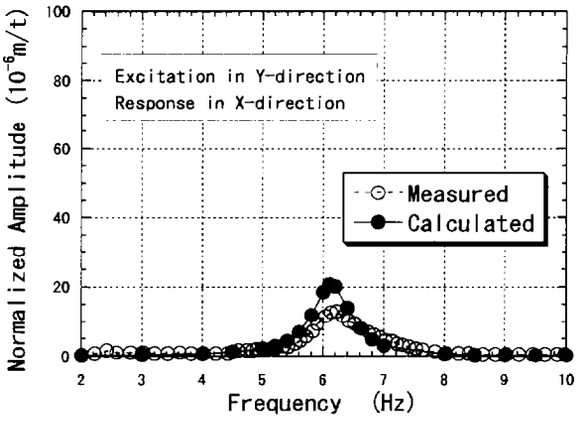

(b) Response in X-direction

Fig.6 Experimental Results of FVT2 and results calculation(quoted from Yamaya et al. (1995) a modified)

DISCUSSION

Features of the results in HLSST

The results of velocity logging, earthquake observation and FVT conducted in HLSST indicate peculiar behavior of the gravelly layer and the model building as follows ;

1) Shear wave velocity by velocity logging varies widely in the gravelly layer (See Fig.4(a)).
2) Shear wave velocity of the gravelly layer identified by inversion analysis shows obvious azimuth dependency (See Fig.4(b)).
3) Each resonance curve by the FVT at Stage 3 has double peaks. Thus, the couple of resonance frequencies of each resonance curve are different from each other (See Figs.5(a) and 5(b)).

In this chapter, the cause of the above-mentioned phenomena and their modeling will be discussed in the following.

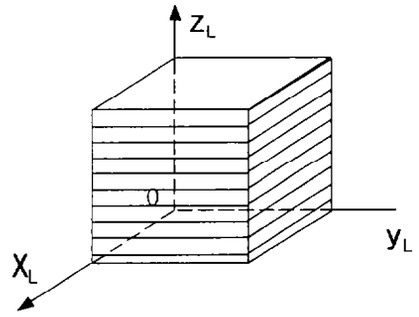

(a) Coordinate system z_L-axis of which is perpendicular to the isotropic plane

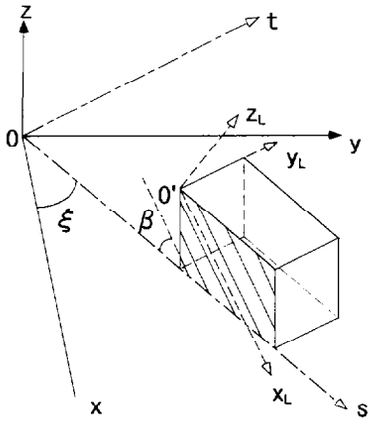

(b) Coordinate system transformed from x_L-y_L-z_L coordinate system

Fig.7 Coordinate system for orthotropic elastic body

Modeling the anisotropic behavior of the gravelly layer by the orthotropic elastic body

In previous report (Tanaka and Okamoto, 1998), I concluded that the azimuth dependency of the gravelly layer, which is the phenomena 2), was attributable that the bedding plane of the inherently anisotropic gravelly layer in the HLSST site was slanted off the horizontal. Thus, stress-strain relationships of the gravelly soil are investigated herein, assuming that the azimuth dependency of shear wave velocity of the gravelly layer is attributable to the inclination of the bedding plane to the horizontal plane.

Modeling the azimuth dependency of shear wave velocity by an orthotropic elastic body

Generally, an orthotropic elastic material has parallel planes on which mechanical characteristics are isotropic. Thus, the plane is called as an isotropic plane in this paper. Assuming that x_L-axis and y_L-axis are parallel to the isotropic plane and that z_L-axis is perpendicular to the isotropic plane as shown in Fig.7(a), stress-strain relationships of the orthotropic elastic body can be expressed by the following equations ;

$$\begin{Bmatrix} \varepsilon_{x_L} & \varepsilon_{y_L} & \varepsilon_{z_L} & \gamma_{y_Lz_L} & \gamma_{z_Lx_L} & \gamma_{x_Ly_L} \end{Bmatrix}^T = \begin{bmatrix} \frac{1}{E_h} & -\frac{\nu_h}{E_h} & -\frac{\nu_{vh}}{E_v} & 0 & 0 & 0 \\ -\frac{\nu_h}{E_h} & \frac{1}{E_h} & -\frac{\nu_{vh}}{E_v} & 0 & 0 & 0 \\ -\frac{\nu_{vh}}{E_v} & -\frac{\nu_{vh}}{E_v} & \frac{1}{E_v} & 0 & 0 & 0 \\ 0 & 0 & 0 & \frac{1}{G_v} & 0 & 0 \\ 0 & 0 & 0 & 0 & \frac{1}{G_v} & 0 \\ 0 & 0 & 0 & 0 & 0 & \frac{1}{G_h} \end{bmatrix} \cdot \begin{Bmatrix} \sigma_{x_L} \\ \sigma_{y_L} \\ \sigma_{z_L} \\ \tau_{y_Lz_L} \\ \tau_{z_Lx_L} \\ \tau_{x_Ly_L} \end{Bmatrix} \quad (1a)$$

$$\frac{1}{E_h} = \frac{1}{2(1+\nu_h)} \cdot \frac{1}{G_h} \quad (1b)$$

where,

E_h : Young's modulus when σ_{xL} or σ_{yL} is applied solely.
E_v : Young's modulus when σ_{zL} is applied solely.
G_v : Shear modulus when τ_{yLzL} or τ_{zLxL} is applied solely.
G_h : Shear modulus when τ_{xLyL} is applied solely.
ν_h : Poisson's ratio defined as $-\varepsilon_{xL}/\varepsilon_{yL}$ ($-\varepsilon_{yL}/\varepsilon_{xL}$) when σ_{yL} (σ_x is applied solely.
ν_{vh} : Poisson's ratio defined as $-\varepsilon_{xL}/\varepsilon_{zL}$ or $-\varepsilon_{yL}/\varepsilon_{zL}$ when σ_{zL} i applied solely.

After coordinate transformation of Eq.(1a) is conducted, the stress-strain relationships of the orthotropic elastic body in x-y-z coordinate system shown in Fig.7(b) are derived.

If the bedding plane is inclined to the direction of U_2-axis (Ueshima and Okano, 1996) shown in Fig.3, the following equations are derived.

$$\frac{1}{G_{yz}} = -\sin^2\xi \cdot \left(\frac{1}{G_{min}} - \frac{1}{G_{max}} \right) + \frac{1}{G_{min}} \quad (2a)$$

$$\frac{1}{G_{zx}} = -\cos^2\xi \cdot \left(\frac{1}{G_{min}} - \frac{1}{G_{max}} \right) + \frac{1}{G_{min}} \quad (2b)$$

where,
G_{min} : the minimum of G_{yz} and G_{zx}
G_{max} : the maximum of G_{yz} and G_{zx}
ξ : Angle between the direction of inclination of the isotropic plane and x-axis (See Figs.3 and 7(b)).

Determining parameters Gmax and Gmin by the results o inversion analysis

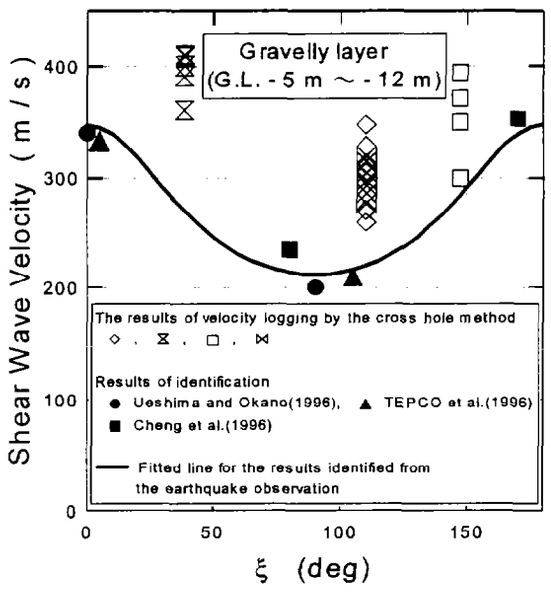

Fig.8 Relationships between ξ and shear wave velocity

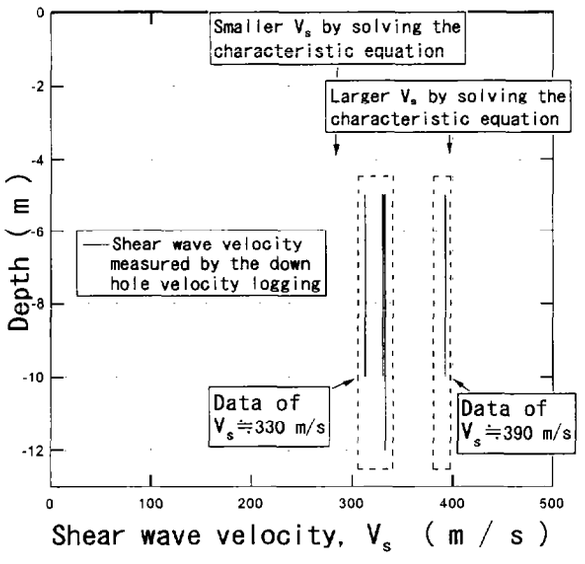

Fig.9 Shear wave velocity by the down hole method (Measured values and calculated values)

The open symbols in Fig.8 show the relationships between shear wave velocity obtained by the in-situ velocity logging by the cross hole method and ξ , assuming that the bedding plane of the gravelly layer is inclined to the direction of U_2-axis in Fig.3. The shear wave velocities identified by the inversion analysis are also plotted as solid symbols in Fig.8. The solid curve in Fig.8 is calculated by Eq.(2b) in which G_{max} and G_{min} are determined by the regression analysis using shear wave

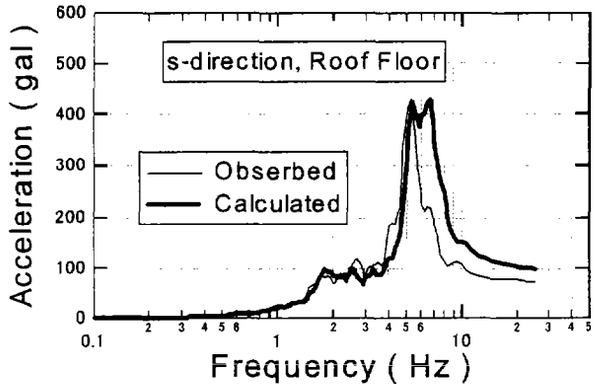

(a) Response in s-direction

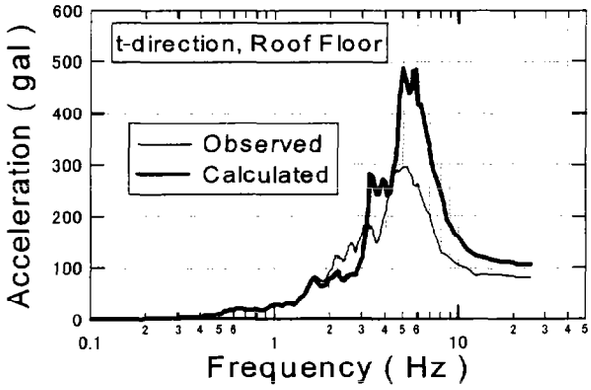

(b) Response in t-direction

Fig.10 Earthquake response (Observed results and calculate results)

velocities identified by the inversion method. The values c G_{max} and G_{min} for the solid line in Fig.8 are 293 MPa and 10 MPa, respectively.

Figure 8 indicates that the azimuth dependency of the gravell layer can be expressed by Eq.(2b) if the parameters ar properly determined. Therefore, the azimuth dependency c the gravelly layer in HLSST site can be modeled by th orthotropic elastic body.

Calculation of Vs by the down-hole velocity logging

Figure 9 shows distribution of shear wave velocities measur by down-hole velocity logging. A closer look at Fig.9 seems reveal that measured shear wave velocities seem to be divid into two groups ; data of about 330 m/s and datum of about 3 m/s.

Two shear wave velocities can be also obtained by solving characteristic equation. These values are also plotted in Fig. The larger value seems to correspond to the datum of $V_s \fallingdotseq 3$ m/s, while the smaller value seems to correspond to the data $V_s \fallingdotseq 330$ m/s. Thus, it can be explained by the orthotro

elastic body model that shear wave velocities measured by down-hole velocity logging were divided into two groups.

Simulation analyses of the forced vibration tests and earthquake response

3-dimensional simulation analyses of the forced vibration tests and earthquake response conducted herein by a computer code "ABAQUS" using the orthotropic elastic model described previously. The properties of soils and boundary conditions for the dynamic analyses are described in literature (Tanaka, 2000).

The experimental results of FVT1 are compared in Figs.5(a) and 5(b) with their simulated results. It can be pointed out that the resonance curves are well simulated. Especially, the whole shape and the double peaks of the simulated curves are very similar to the experimental results. The experimental results of FVT2 are compared in Figs.6(a) and 6(b) with their simulated results. It can be also pointed out that the resonance curves are well simulated. Especially, the whole shape and the single peaks of the simulated curves are very similar to the experimental results.

The results of earthquake response are compared in Figs.10(a) and 10(b) with their simulated results. Though the observed results are simulated by the analyses approximately, the accuracy is not satisfactory. According to Figs.10(a) and 10(b), calculated peak frequencies are larger than observed peak frequencies. This is attributable to the effect of nonlinearity on the observed earthquake response. According to Figs.10(a) and 10(b), calculated peak acceleration is larger than observed one. This seems to be related to evaluation of damping ratio for earthquake response analysis (Tanaka, 2000).

CONCLUSIONS

(1) The azimuth dependency of the shear wave velocity measured by the cross-hole velocity logging can be expressed by the orthotropic elastic body model.
(2) It can be explained by the orthotropic elastic body model that shear wave velocities measured by down-hole velocity logging were divided into two groups.
(3) The resonance curves of horizontal forced vibration tests of the model building with or without backfill can be successfully simulated by the orthotropic elastic model. Moreover, the orthotropic elastic model can simulate results of earthquake response.

ACKNOWLEDGMENTS

The author is grateful to Prof. T. Kokusho (Chu-oh University), Dr. K. Nishi (CRIEPI), Dr. T. Ueshima (CRIEPI) and Dr. T. Okamoto (CRIEPI) for useful advice about the HLSST. The author is also grateful to Mr. K. Nakazono (D.C.C. Co., Ltd.) for conducting numerical analysis.

REFERENCES

Chen, C.H., Yeh, C.S., Lee, Y.J. and Chiou, H.J. [1996] Seismic ground responses of Hualien LSST site, a paper fron Taiwan Power Company Group submitted to the Hualier LSST Project Meeting.

Kokusho, T., Nishi, K., Okamoto, T., Tanaka, Y., Ueshima, T Kudo, K., Kataoka, T., Ikemi, M., Kawai, T., Sawada, Y. Suzuki, K. and Yajima, K. [1997]. Distribution of grounc rigidity and ground model for seismic response analysis ir Hualien project of large scale seismic test, Nuclea Engineering and Design, Vol.172, pp. 297-308.

Morishita, H., Tanaka, H., Nakamura, N., Kobayashi, T., Kan S., Yamaya, H. and Tang, H.T. [1993]. Forced vibration tes of the Hualien large scale SSI model, SMiRT-12, K02/1 Elsevier Science Publishers B.V. , pp. 37-42.

Sugawara, Y., Uetake, T., Kobayashi, T. and Yamaya, H [1997]. Forced vibration test of the Hualien large scale soi structure interaction model (part 2), Nuclear Engineering anc Design, Vol.172, pp. 273-280.

Tanaka, Y. and Okamoto, T. [1998]. Anisotropy anc heterogeneity of gravelly soil layer in Hualien, Taiwan, The Geomechanics of Hard Soils – Soft Rocks, Balkema, pp. 889 – 900.

Tanaka, Y. [2000]. Hualien large scale seismic test f soil-structure interaction research, – Dynamic simulatic analysis using orthotropic elastic body –, Report of Centr Research Institute of Electric Power Industry, No.U99038. (Japanese)

TEPCO Group and Kajima Research Institute [1996] Optimum soil profile for L and T component, a paper submitted to the Hualien LSST Project Meeting.

Ueshima, T. and Okano, H. [1996]. Further investigation o seismic response of soil and embedded structure in Hualier LSST program, Proc. of 11th World Conference or Earthquake Engineering, Paper No.1930, Elsevier Science Ltd., 1996.

Ueshima, T., Kokusho, T., Okamoto, T. and Yajima, H [1997]. Seismic response analysis of embedded structure a Hualien, Taiwan, Nuclear Engineering and Design, Vol.172 pp.289-295.

Yamaya, H., Kobayashi, T. and T. Sugiyama, T. [1995]. Study on forced vibration tests, Test results and their analysis, J. Struct. Constr. Eng., AIJ, No.478, pp. 81-90. (In Japanese)